Optimal Resistive Elements for Multiple Mode Shunt Damping of a Piezoelectric Laminate Beam

Sam Behrens & S. O. Reza Moheimani
Department of Electrical and Computer Engineering
The University of Newcastle NSW 2308 Australia
{sbehrens,reza}@ee.newcastle.edu.au

Abstract

In this paper a methodology that addresses the problem of choosing optimal resistive elements for multiple mode shunt damping of a piezoelectric laminate is presented. The proposed method is based on the H_2 norm optimization for the composite system, and is validated through experimental work on a piezoelectric laminated simply-supported beam.

1 Introduction

Today's increasingly high speed and light weight structures are subject to extensive vibrations that diminish their structural life, or in the worst case, lead to a catastrophic failure. In order to prevent these effects, one solution is passive shunt damping. This technique has been widely applied [3, 4, 5, 6, 10, 11], and is regarded as a simple, low-cost, light-weight, easy-to-implement, and guaranteed to be *stable* [1] method for controlling structural vibration.

A current area of research is dealing with the implementation of a single piezoelectric sensing element capable of multiple mode shunt damping. This method, presented in references [6, 11, 12, 13, 14], uses a fixed impedance structure for the shunt circuits. In reference [12] the author reports a method for piezoelectric shunt damping of multiple vibration modes using a single piezoelectric transducer (PZT). The method differs from other multiple mode shunting schemes, see for example [3, 6], in that a "blocking" circuit is used. Even though this technique is reliable and the complete circuit can be fine-tuned by trial and error [3, 4, 6, 11, 12, 13, 14], there are two important questions that need to be addressed when applying multiple mode shunt damping. The first question is how the shunt resistive values required for optimal multi-mode shunting should be calculated. The second question, is why the parallel shunt damping case presented in [11, 12, 13, 14], is easier to implement practically than the series shunting circuit [3, 4, 6]. It is, therefore, the aim of this paper to present answers to these two questions.

Current techniques for determining the resistive elements for shunt damping are based on rather ad-hoc methodologies. It is hoped that this work will develop a more systematic way of calculating these resistive elements in an optimal way. Furthermore, the method of this paper can be extended to allow for shunt damping of a structure using several piezoelectric devices.

The theoretical ideas presented are justified by experimental verification performed on a piezoelectric laminated simply-supported beam for two structural modes.

The paper is organized as follows. In Section 2, the dynamics of a piezoelectric laminated beam system is modeled. In Section 3, the composite model of the shunt circuit and the piezoelectric laminated beam is developed. An optimization procedure is presented in Section 4 for obtaining the optimal resistive elements for a multi-mode shunt circuit. In Section 5, some experimental results on a piezoelectric laminated beam are proposed using optimal resistive values by the direct application of the theory introduced in the Section 4. And finally in Section 6, the paper is concluded.

2 Dynamical Model of the Composite System

Consider the simply-supported piezoelectric laminate beam in Figure 1. A pair of piezoelectric patches are bonded to the host structure. One piezoelectric layer will be used as an actuator and the other for passive shunting.

The differential equation describing the elastic deflection of the composite beam is the modified one dimensional Bernoulli-Euler beam equation [1]. By using the *modal analysis technique* [7] the position function $y(x,s)$, can be expanded as an infinite series. Using the appropriate boundary conditions for a simply-supported beam, we can determine the resonant frequencies ω_i and mode shapes ϕ_i according to the specified orthogonality conditions [7].

When modeling the dynamics of the composite system, illustrated in Figure 1, it is necessary to derive the transfer function between the displacement at any point along the beam and the actuator voltage, i.e. $Y(x,s)/V_a(s)$ [8], and between the shunting piezoelectric voltage and the actuator voltage $V_s(s)/V_a(s)$ [8]. Both transfer functions are stated

[1] In contrast with active control which may present some stability problems.

below;

$$\frac{Y(x,s)}{V_a(s)} = \sum_{i=1}^{\infty} \frac{C_a[\phi_i'(x_1) - \phi_i'(x_2)]\phi_i(x)}{s^2 + 2\zeta_i\omega_i s + \omega_i^2} \quad (1)$$

$$\frac{V_s(s)}{V_a(s)} = \sum_{i=1}^{\infty} \frac{C_s C_a[\phi_i'(x_1) - \phi_i'(x_2)][\phi_i'(x_3) - \phi_i'(x_4)]}{s^2 + 2\zeta_i\omega_i s + \omega_i^2}. \quad (2)$$

C_a, C_s are the piezoelectric constants associated with the actuator and shunting layer [1]. Note that the additional term $2\zeta_i\omega_i s$, is added to compensate for structural damping and is usually determined experimentally.

Then state-space model for $Y(x,s)/V_a(s)$ and $V_s(s)/V_a(s)$ can be represented as

$$\dot{\mathbf{x}}_b = \mathbf{A}\mathbf{x}_b + \mathbf{B}V_a \quad (3)$$
$$Y = \mathbf{C}_Y\mathbf{x}_b \quad (4)$$
$$V_s = \mathbf{C}_{V_s}\mathbf{x}_b \quad (5)$$

where $\mathbf{x}_b$ is the beam states, $\mathbf{C}_Y$ and $\mathbf{C}_{V_s}$ depend on the $Y(x,s)$ and $V_s(s)$.

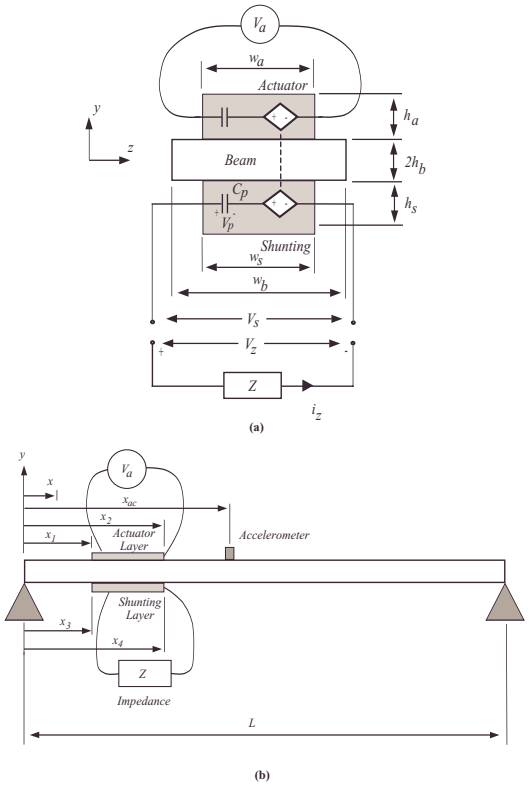

Figure 1: (a) Cross-section of the beam with piezoelectric laminate present; and (b) The piezoelectric laminated simply-supported beam.

3 Modeling the Passive System

From previous reports [11, 12, 13, 14], the authors assume a fixed circuit structure for multi-mode shunt damping. There are two different multi-mode shunt structures: (1) parallel shunt circuit; and (2) series shunt circuit. Examples of these two cases are shown in Figures 2 and 3.

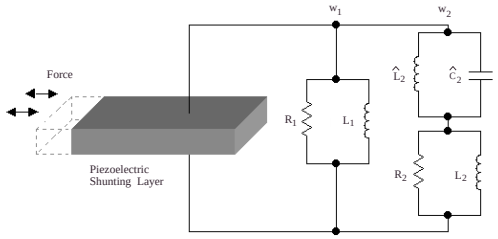

Figure 2: Parallel shunt circuit case for shunt damping two modes at ω_1 and ω_2.

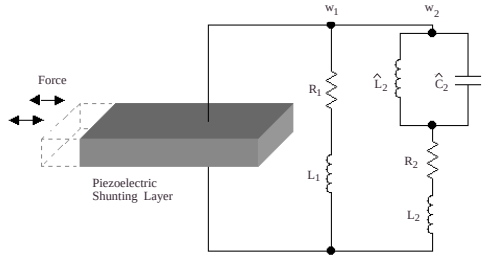

Figure 3: Series shunt circuit case for shunt damping two modes at ω_1 and ω_2.

For the simple cases depicted in Figures 2 and 3 where two modes are to be shunt-damped, the "blocking" circuit [12] is connected in series with the shunting branch R_2-L_2 in each case. The "blocking" circuit is the parallel capacitor-inductor, $\hat{C}_2$-$\hat{L}_2$. The number of antiresonant circuits in each *R-L* shunting branch depends on the number of structural modes to be shunt damped simultaneously. Each *R-L* shunting branch is designed to dampen only one structural mode. For example, the R_1-L_1 branches, in both figures are tuned at the ω_1 structural mode, while the branches R_2-L_2 are tuned at the ω_2 structural mode.

In order to model the presence of the shunt dampener on the resonant structure, the composite system dynamics need to be considered. Piezoelectric transducers behave electrically like a capacitor C_p and mechanically like a stiff spring. It is common to model the piezoelectric element as a capacitor C_p in series with a voltage source which is dependent on the dynamics of the resonant structure [5]. Consider Figures 1 and 4, where a piezoelectric patch is shunted by an impedance Z. Hence, the current-voltage relation of the impedance can be represented in state-space form as

$$\dot{\mathbf{x}}_z = \mathbf{A}_z\mathbf{x}_z + \mathbf{B}_z V_z \quad (6)$$
$$i_z = \mathbf{C}_z\mathbf{x}_z + \mathbf{D}_z V_z \quad (7)$$

where V_z is the voltage across the impedance and i_z is the current flowing through the circuit with the obvious definition for $\mathbf{A}_z$, $\mathbf{B}_z$, $\mathbf{C}_z$ and $\mathbf{D}_z$. The relationship between the V_z

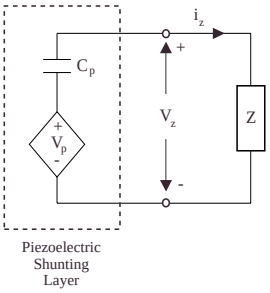

Figure 4: Schematic of piezoelectric shunting layer with a shunting impedance Z present.

and V_p, shown in Figures 1 and 4, is

$$\dot{\mathbf{x}}_b = \mathbf{A}\mathbf{x}_b + \mathbf{B}V_z \quad (8)$$

$$V_p = -\mathbf{C}_{V_s}\mathbf{x}_b \quad (9)$$

where V_p is the voltage induced from the electromechanical coupling effect, due to the dynamics of the resonant structure. By shunting the piezoelectric patch, the voltage V_z across the shunting layer or impedance, shown in Figure 4, is related to the other magnitude as,

$$V_z = V_p - \frac{1}{C_p}\int i_z dt \quad (10)$$

where C_p represents capacitance of the shunting layer. The variable i_z, in turn, can be replaced by the $\dot{\mathbf{q}}_z$, which is the charge across the shunting piezoelement. Consequently, replacing V_z and using $V_p = -\mathbf{C}_{V_s}\mathbf{x}_b$ then (6), (7) and (8) becomes,

$$\begin{bmatrix} \dot{\mathbf{x}}_b \\ \dot{\mathbf{x}}_z \\ \dot{\mathbf{q}}_z \end{bmatrix} = \begin{bmatrix} \mathbf{A}-\mathbf{B}\mathbf{C}_{V_s} & \mathbf{0} & -\frac{1}{C_p}\mathbf{B} \\ -\mathbf{B}_z\mathbf{C}_{V_s} & \mathbf{A}_z & -\frac{1}{C_p}\mathbf{B}_z \\ -\mathbf{D}_z\mathbf{C}_{V_s} & \mathbf{C}_z & -\frac{1}{C_p}\mathbf{D}_z \end{bmatrix} \begin{bmatrix} \mathbf{x}_b \\ \mathbf{x}_z \\ \mathbf{q}_z \end{bmatrix}. \quad (11)$$

If a voltage is applied to the actuator piezoelement patch V_a i.e. the compound system, then (11) becomes,

$$\dot{\mathbf{X}} = \tilde{\mathbf{A}}\mathbf{X} + \tilde{\mathbf{B}}V_a \quad (12)$$

$$V_z = \tilde{\mathbf{C}}_{V_s}\mathbf{X} \quad (13)$$

$$Y = \tilde{\mathbf{C}}_Y\mathbf{X}. \quad (14)$$

where $\mathbf{X} = \begin{bmatrix} \mathbf{x}_b & \mathbf{x}_z & \mathbf{q}_z \end{bmatrix}^T$, $\tilde{\mathbf{B}} = \begin{bmatrix} \mathbf{B} & \mathbf{0} & \mathbf{0} \end{bmatrix}^T$, $\tilde{\mathbf{C}}_{V_s} = \begin{bmatrix} \mathbf{C}_{V_s} & \mathbf{0} & \mathbf{0} \end{bmatrix}^T$, $\tilde{\mathbf{C}}_Y = \begin{bmatrix} \mathbf{C}_Y & \mathbf{0} & \mathbf{0} \end{bmatrix}^T$ and

$$\tilde{\mathbf{A}} = \begin{bmatrix} \mathbf{A}-\mathbf{B}\mathbf{C}_{V_s} & \mathbf{0} & -\frac{1}{C_p}\mathbf{B} \\ -\mathbf{B}_z\mathbf{C}_{V_s} & \mathbf{A}_z & -\frac{1}{C_p}\mathbf{B}_z \\ -\mathbf{D}_z\mathbf{C}_{V_s} & \mathbf{C}_z & -\frac{1}{C_p}\mathbf{D}_z \end{bmatrix}.$$

4 Optimization

In order to find the appropriate values for resistors R_i, an optimization approach is proposed. A set of resistors can be found such that the H_2 norm of the combined system is minimized. Since flexible structures are highly resonant systems, their frequency response consist of very sharp resonant peaks. By minimizing the H_2 norm of the combined system, these peaks can be pushed down. This is due to the fact that the H_2 norm of the system is related to the area under its magnitude response.

Consider a transfer function matrix $\tilde{\mathbf{G}}(s)$ for the compounded system, i.e. include the passive controller. Then the H_2 norm of $\tilde{\mathbf{G}}(s)$, denoted $\left\|\tilde{\mathbf{G}}(s)\right\|_2$, is defined as:

$$\left\|\tilde{\mathbf{G}}(s)\right\|_2^2 = \frac{1}{2\pi}\int_{-\infty}^{\infty} tr\left\{\tilde{\mathbf{G}}^T(-j\omega)\tilde{\mathbf{G}}(j\omega)\right\} d\omega. \quad (15)$$

Let also $\tilde{\mathbf{G}}(s)$ have the realization $\tilde{\mathbf{G}}(s) = \tilde{\mathbf{C}}(s\mathbf{I} - \tilde{\mathbf{A}})^{-1}\tilde{\mathbf{B}}$. Then if the matrix $\tilde{\mathbf{A}}$ is stable, the following equality holds

$$J = \|\mathbf{G}(s)\|_2^2 = tr(\tilde{\mathbf{C}}\mathbf{P}\tilde{\mathbf{C}}^T) \quad (16)$$

where $\mathbf{P}$ satisfies the *Lyapunov* equation $\tilde{\mathbf{A}}^T\mathbf{P} + \mathbf{P}\tilde{\mathbf{A}} + \tilde{\mathbf{B}}\tilde{\mathbf{B}}^T = \mathbf{0}$. Since $\tilde{\mathbf{A}}$ is a function of R_i, the following unconstrained optimization problem needs to be solved:

$$R_i^* = \arg\ \min\ J. \quad (17)$$

We could use a direct search method optimization algorithm (Nelder-Mead Simplex) but a more elegant method of obtaining the optimal resistance R_i, is to set up gradient search algorithm. The optimization problem (17) can then be written as a constrained optimization problem, as

$$R_i^* = \arg \min_{s.t.\ \mathbf{g}=\mathbf{0},\ R_i>0} J \quad (18)$$

where $\mathbf{g} = \tilde{\mathbf{A}}^T\mathbf{P} + \mathbf{P}\tilde{\mathbf{A}} + \tilde{\mathbf{B}}\tilde{\mathbf{B}}^T$. To solve this constrained optimization problem, we need to introduce Lagrange multipliers $\mathbf{S}$ and form the Lagrangian L as follows

$$L = tr(\tilde{\mathbf{C}}\mathbf{P}\tilde{\mathbf{C}}^T) + tr(\mathbf{g}\mathbf{S}). \quad (19)$$

It is necessary to determine the conditions for optimality by taking the derivatives of L, with respect to parameters $\mathbf{P}$, $\mathbf{S}$ and R_i and setting the derivatives to zero,

$$\frac{\partial L}{\partial \mathbf{S}} = \tilde{\mathbf{A}}\mathbf{P} + \mathbf{P}\tilde{\mathbf{A}}^T + \tilde{\mathbf{B}}\tilde{\mathbf{B}}^T = \mathbf{0} \quad (20)$$

$$\frac{\partial L}{\partial \mathbf{P}} = \tilde{\mathbf{A}}^T\mathbf{S} + \mathbf{S}\tilde{\mathbf{A}} + \tilde{\mathbf{C}}^T\tilde{\mathbf{C}} = \mathbf{0} \quad (21)$$

$$\frac{\partial L}{\partial R_1} = tr\left(\tilde{\mathbf{E}}_1\mathbf{P}\mathbf{S} + \mathbf{P}\tilde{\mathbf{E}}_1^T\mathbf{S}\right) = 0 \quad (22)$$

$$\vdots$$

$$\frac{\partial L}{\partial R_k} = tr\left(\tilde{\mathbf{E}}_k\mathbf{P}\mathbf{S} + \mathbf{P}\tilde{\mathbf{E}}_k^T\mathbf{S}\right) = 0. \quad (23)$$

Assuming k resistors, we can represent $\tilde{\mathbf{A}}$ as $\hat{\mathbf{A}} + \sum_{i=1}^{k} R_i\tilde{\mathbf{E}}_i$ where matrix $\hat{\mathbf{A}}$ is not a function of R_i. By factoring out R_i from matrix $\tilde{\mathbf{E}}_i$ this allows us to perform differentiation, as in (22) and (23).

To find the minimum H_2 norm of the system, the above relationships have to be solved simultaneously. It is not possible to obtain a closed form solution, so a numerical approach is required.

The optimization procedure starts with an initial guess for each resistor R_i, such that $R_i > 0$. Matrices $\tilde{\mathbf{B}}$ and $\tilde{\mathbf{C}}$ only need to be calculated once, because they are independent of R_i. Matrix $\tilde{\mathbf{A}}$ is a function of R_i which needs to be updated for each iteration (j). While matrices $\mathbf{P}$ and $\mathbf{S}$, are calculated by solving the Lyapunov equations in (20) and (21). The gradient for each value of R_i^j is calculated from (22) and (23) and is used to find the steepest descent. The process is iterated by updating R_i until an optimal solution is obtained (i.e. until sufficient exiting conditions are obtained $\frac{\partial L^j}{\partial R_i} \approx 0$ and $L^{j+1} \approx L^j$). Since the problem is not convex, an iterative optimization procedure can be carried out for a number of initial guesses to obtain the best solution.

5 Experimental Verification

To validate the concepts presented, experiments were carried out on a simply-supported piezoelectric laminated beam. The experimental setup is displayed in Figure 1. The beam structure consists of a uniform aluminum beam of a rectangular cross section. Refer to Table 1 for beam parameters. The beam is experimentally pinned at both ends and *ideal* boundary conditions are assumed. A pair of piezoelectric ceramic patches are attached symmetrically to either side of the beam, at $0.05m$ from one of the pinned ends, i.e. $x_1 = x_3 = 0.05m$. The piezoceramic elements used on the experimental composite structure are PIC151 patches. The physical parameters for the piezoelectric patch PIC151 are given in Table 2.

Length, L	$0.6m$
Width, w_b	$0.05m$
Thickness, h_b	$0.003m$
Youngs Modulus, E_b	$65 \times 10^9 N/m^2$
Density, ρ	$2650 kg/m^2$

Table 1: Parameters of the simply-supported beam.

Charge Constant, d_{31}	$-210 \times 10^{-12} m/V$
Voltage Constant, g_{31}	$-11.5 \times 10^{-3} Vm/N$
Coupling Coefficient, k_{31}	0.340
Capacitance, C_p	$0.105 \mu F$
Width, w_s w_a	$0.025m$
Thickness, h_s h_a	$0.25 \times 10^{-3} m$
Youngs Modulus, E_s E_a	$63 \times 10^9 N/m^2$

Table 2: Parameters of the PIC151 piezoelectric patches.

During the experiment, the simply-supported beam was excited using the piezoelectric actuator layer with a swept sine source from a Hewlett Packard 35670A signal analyzer. The swept sine signal was then amplified using a high voltage power amplifier. To find the transfer function $V_s(s)/V_a(s)$, the input channel of the signal analyzer was used to measure the voltage across the sensing piezoelectric layer. Using a Brüal & Kjaer accelerometer and Nexus conditional amplifier the $Y(x,s)/V_a(s)$ transfer function was determined for a point on the composite structure located at $x_{ac} = 0.170m$. The response for $V_s(s)/V_a(s)$ and $Y(x,s)/V_a(s)$ was captured by the signal analyzer. The results are displayed in Figure 5, for the first five modes.

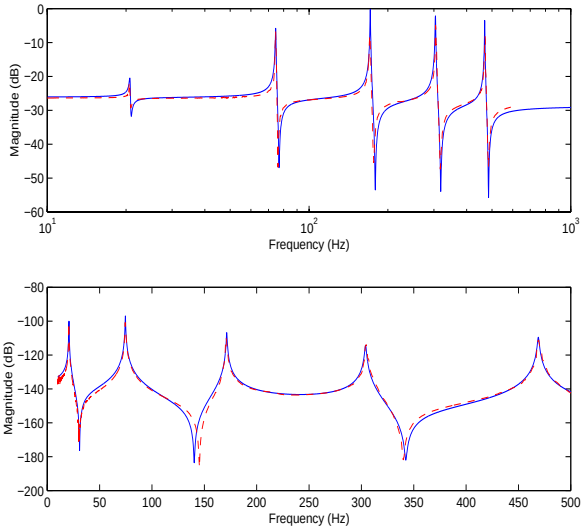

Figure 5: Frequency response: (a) $V_s(s)/V_a(s)$, (b) $Y(x,s)/V_a(s)$ where $x_{ac} = 0.170m$ from the pinned boundary of the composite beam. Simulated (—) and experimental results ($\cdots$).

The piezoelectric composite system was modeled using a model order of 5, with the appropriate feedthrough term [8, 2]. From Figure 5, it can be observed that the theoretical model describes very well the behaviour of the system. From the measured response, several structural vibration modes can be observed. The first five resonant modes for the simply-supported beam were at 19.7, 74.8, 169.4, 300, and $468Hz$.

Two different shunt circuits were examined, they are: (1) parallel shunt circuit; and (2) series shunt circuit. Also, for simplicity only the $2nd$ ($\omega_1 = 74.8Hz$) and $3rd$ ($\omega_2 = 169.4Hz$) structural modes of the piezoelectric composite beam were considered for shunting. The $2nd$ and $3rd$ structural modes were chosen due to their high resonant amplitudes, as shown in Figure 5. The reason for only considering the $2nd$ and $3rd$ mode is because these modes have more authority in comparison to other structural modes due to the chosen location of the piezoelectric patch.

According to [12], the two mode shunting circuits can be simplified using classical circuit theory to the forms shown in Figure 2 and 3, and the inductance (L_1, L_2 and $\hat{L}_2$) of these

two circuits are defined as follows,

$$L_1 = \frac{1}{\omega_1^2 C_p} \quad \tilde{L}_2 = \frac{1}{\omega_2^2 C_p} \quad \hat{L}_2 = \frac{1}{\omega_1^2 \hat{C}_2} \tag{24}$$

$$L_2 = \frac{\left(L_1\tilde{L}_2 + \tilde{L}_2\hat{L}_2 - L_1\hat{L}_2 - \omega_2^2 L_1\tilde{L}_2\hat{L}_2\hat{C}_2\right)}{\left(L_1 - \tilde{L}_2\right)\left(1 - \omega_2^2\hat{L}_2\hat{C}_2\right)}. \tag{25}$$

Both parallel and series circuit cases were designed under the assumption that $\omega_1 < \omega_2$.

The capacitance parameter $\hat{C}_2$, for the "blocking" circuit was chosen to be $100nF$ because of commercial availability of these capacitors. From (25) the inductor parameters were found to be $L_1 = 43H$, $L_2 = 20.9H$, and $\hat{L}_2 = 45.2H$. Using the already mentioned circuit parameters for the shunt and dynamic composite modeling method, the H_2 norm of the composite system was minimized. The optimal resistance values for R_1 and R_2, for both parallel and series shunt cases are obtained. Figure 6 and 7 show the H_2 norm cost surface as a function of R_1 and R_2.

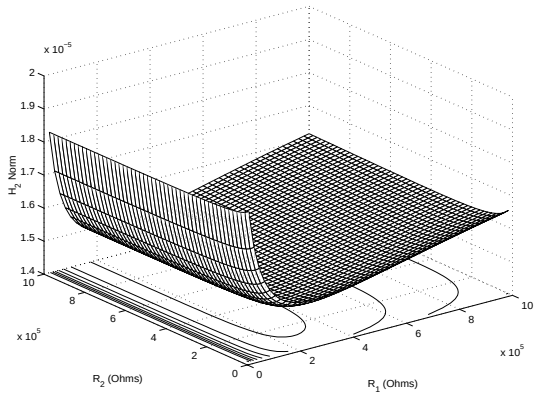

Figure 6: Parallel shunt circuit case, H_2 norm cost surface as a function of R_1 and R_2.

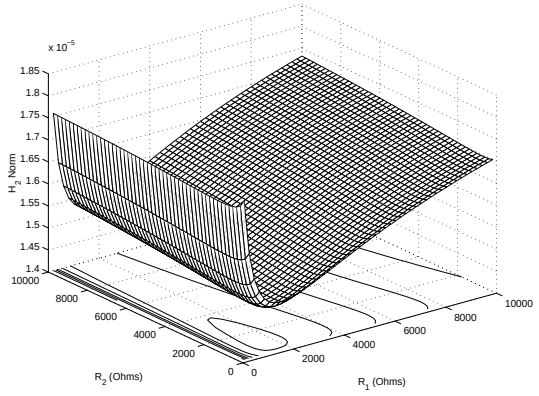

Figure 7: Series shunt circuit case, H_2 norm cost surface as a function of R_1 and R_2.

From Figures 6 and 7, it can be seen that both cost surfaces have a minimum. For the parallel shunt case, the optimal region is larger than the one for the series shunt case. This justifies the work presented in [11], which states that *"the parallel shunt circuit is therefore easier and more practical"* i.e. the parallel shunt case is less sensitive to circuit tuning compared with the series case.

The optimization algorithm found a minimum at $R_1 = 262.75k\Omega$ and $R_2 = 550.73k\Omega$ for the parallel shunt case, while the minimum for the series shunt case was found to be at $R_1 = 1543.4\Omega$ and $R_2 = 1145.2\Omega$.

Parameters R_1, R_2, L_1, L_2, $\hat{L}_2$ and $\hat{C}_2$ were then employed in the design of the two shunt circuits, parallel and series shunt case, and then tested across the piezoelectric patch. Construction of the shunt circuits requires Riodan high Q factor simulated floating/grounded inductors [9], for L_1, L_2 and $\hat{L}_2$.

To justify the H_2 norm optimization technique, the magnitude frequency response were taken for the $Y(x,s)/V_a(s)$ before and after shunt damping at $x_{ac} = 0.170m$. Figures 8 and 9 show the results for parallel and series circuit cases respectively.

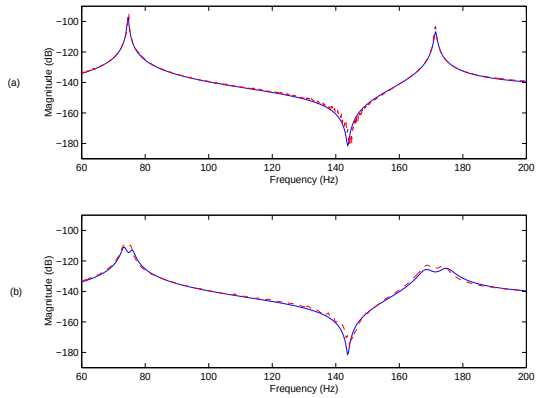

Figure 8: Parallel shunt circuit case, magnitude frequency response for $Y(x,s)/V_a(s)$ where $x_{ac} = 0.170m$ from one pinned end. (a) Undamped and (b) damped where (—) and $(\cdots)$ represent simulated and experimental results respectively.

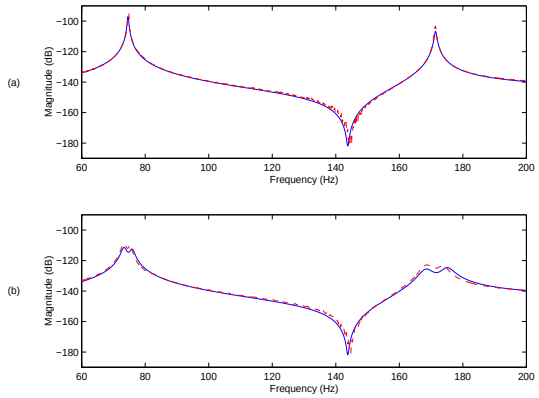

Figure 9: Series shunt circuit case, magnitude frequency response for $Y(x,s)/V_a(s)$ where $x_{ac} = 0.170m$ from one pinned end. (a) Undamped and (b) damped where (—) and $(\cdots)$ represent simulated and experimental results respectively.

After tuning the shunt resistances the following experimental values were found; parallel multi-mode shunt case $R_1 = 273.8k\Omega$ and $R_2 = 543.1k\Omega$; and series multi-mode shunt case $R_1 = 1533.2\Omega$ and $R_2 = 1132.4\Omega$. Comparing resistors experimental results with the theoretical results, it can be seen that the experimental tuned values are close to the predicated theoretical optimal values.

The experimental resonant amplitudes for the 2*nd* and 3*rd* modes were successfully reduced for both parallel and series case. The parallel resonant amplitudes were reduced by $14.4dB$ and $19.4dB$. For the series case a reduction of $14.8dB$ and $19.5dB$ was obtained. From theoretical simulations the resonant amplitudes at 2*nd* and 3*rd* modes for both parallel and series circuit case were, $16.1dB$ and $21.4dB$; and $16.4dB$ and $21.9dB$ respectively.

6 Conclusions

An optimization based method for obtaining the optimal resistances for multi-mode shunt damping was presented. The method is intended to solve the difficulties encountered in previous multi-mode damping [12, 13]. By using this technique, it is possible to determine the required resistances and/or a starting point for fine-tuning of the shunt circuits in a systematic manner. The optimization technique provides an easy and reliable way of obtaining the optimal resistance for multi-mode damping. It also eliminates the tedious trial and error method of obtaining the optimal shunt resistance [4, 3, 6, 11, 14, 12, 13].

From the cost surfaces, it is clear that the parallel shunt circuit case is less sensitive to resistance tuning than the series circuit case, this is due to relative flatness of the cost function close to a minimum. This justifies the experimental work presented in [11], that the *"parallel case is more practical for circuit tuning"*.

In the experiments, two multi-mode shunt circuits, namely the parallel and series shunt, of a piezoelectric laminated simply-supported beam were implemented. The experimental results were very successful. Even though only two multi-mode shunting were incorporated, the optimization technique can be forwardly extended to more modes.

A distinct characteristic of this technique is that it can be easily extended to the case when several piezoelectric patches are to be shunt damped on the same resonant structure.

7 Acknowledgments

The authors wish to acknowledge Mr. Andrew Fleming and Mr. Tristan Perez for their assistance in this work. This research was supported by the Centre for Integrated Dynamics and Control (CIDAC) and the Australian Research Council (ARC).

References

[1] S. J. Elliott C. R. Fuller and P. A. Nelson. *Active Control of Vibration*. Academic Press, 1996.

[2] R. L. Clark. Accounting for out-of-bandwidth modes in the assumed modes approach: Implications on colocaled output feedback control. *Journal of Dynamic Systems, Measurement, and Control*, 119:390–395, 1997.

[3] C. M. Fuller et. al. Theoretical and experimental studies of a truss incorporating active members. *Journal of Intelligent Materials Systems and Structures*, 3:333, 1992.

[4] N. W. Hagood and E. F. Crawley. Experimental investigations of passive enhancement of damping space structures. *Journal of Guidance, Control and Dynamics*, 14(6):1100, 1991.

[5] N. W. Hagood and A. Von Flotow. Damping of structure vibrations with piezoelectric materials and passive electrical networks. *Journal of Sound and Vibration*, 14(2):243, 1991.

[6] J. J. Hollkamp. Multimode passive vibration suppression with piezoelectric materials and resonant shunts. *Journal of Intelligent Materials Systems and Structure*, 5:4, 1994.

[7] L. Meirovitch. *Elements of Vibration Analysis*. McGraw-Hill, Sydney, 2nd edition, 1996.

[8] S.O.R. Moheimani. Minimizing the effect of out of bandwidth modes in the truncated assumed modes of structures. *Proc. American Control Conference*, pages 2718–2722, 1999.

[9] R. H. S. Riodan. Simulated inductors using differential amplifiers. *Electron. Lett.*, 3(2):50–51, 1967.

[10] K. W. Wang. Structural vibration suppression via parametric control actions - piezoelectric materials with real-time semi-active networks. *Series on Stability, Vibration and Control of Structures*, 1:112–134, 1995.

[11] S. Y. Wu. Piezoelectric shunts with parallel R-L circuit for smart structural damping and vibration control. *Proceedings of the International Society for Optical Engineering*, 2720:259–269, March 1996.

[12] S. Y. Wu. Method for multiple mode shunt damping of structural vibration using a single pzt transducer. *Proceedings SPIE: Smart Structure and Materials 1993: Smart Structures and Intelligent System*, 3327:159–168, March 1998.

[13] S. Y. Wu. Multiple PZT transducer implemented with multiple-mode piezoelectric shunt for passive vibration damping. *Proceedings SPIE: Smart Structures and Materials 1999: Passive Damping and Isolation*, 3672:112–122, March 1999.

[14] S. Y. Wu and A. S. Bicos. Structure vibration damping experiments using improved piezoelectric shunts. *Proceedings of the International Society for Optical Engineering*, 3045:40–50, March 1997.